

# Effect of Confinement on the Bearing Capacity and Settlement of Spread Foundations

Tahsin Toma Sabbagh, Ihsan Al-Abboodi, Ali Al-Jazaairry

**Abstract**—Allowable-bearing capacity is the competency of soil to safely carries the pressure from the superstructure without experiencing a shear failure with accompanying excessive settlements. Ensuring a safe bearing pressure with respect to failure does not tolerate settlement of the foundation will be within acceptable limits. Therefore, settlement analysis should always be performed since most structures are settlement sensitive. When visualising the movement of a soil wedge in the bearing capacity criterion, both vertically and horizontally, it becomes clear that by confining the soil surrounding the foundation, both the bearing capacity and settlement values improve. In this study, two sizes of spread foundation were considered; (2×4) m and (3×5) m. These represent two real problem case studies of an existing building. The foundations were analysed in terms of dimension as well as position with respect to a confining wall (i.e., sheet piles on both sides). Assuming B is the least foundation dimension, the study comprised the analyses of three distances; (0.1 B), (0.5 B), and (0.75 B) between the sheet piles and foundations alongside three depths of confinement (0.5 B), (1 B), and (1.5 B). Nonlinear three-dimensional finite element analysis (ANSYS) was adopted to perform an analytical investigation on the behaviour of the two foundations contained by the case study. Results showed that confinement of foundations reduced the overall stresses near the foundation by 65% and reduced the vertical displacement by 90%. Moreover, the most effective distance between the confinement wall and the foundation was found to be 0.5 B.

**Keywords**—Bearing capacity, cohesionless soils, spread footings, soil confinement, soil modelling.

## I. INTRODUCTION

ANY foundation when designed should satisfy two essential requirements; first, it must have at least a certain specified safety against bearing capacity failure, and second, the settlement under working load must not exceed the tolerable limits for the superstructure.

In any specific case, one of these criteria will determine the necessary dimensions of the foundation, but it may be difficult to say in advance, which one it will be. Therefore, it is usually necessary to investigate both. The study of ultimate bearing capacity has the purpose of determining the load under which a foundation with given shape, dimensions, and depth sinks indefinitely into the soil. The study of the limit of deformation has the purpose of determining load movements of the structure are at the limit of what is still allowable for the stability.

Fig. 1 shows the pattern of particle motion at failure for a

shallow foundation. This provides the basis for understanding the development of failure in granular soil. When the soil fails, the particles move downward and move in the horizontal direction at the same time. Hence, the soil is pushed out from beneath the footing and the surface of the surrounding soil heaves.

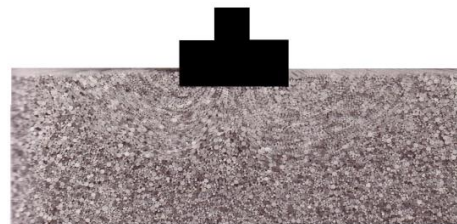


Fig. 1 Failure Zones under Footing (after [1])

By observing the behaviour of shallow foundations subjected to vertical loads, it is a well-established fact that the bearing capacity failure occurs usually as a shear failure of the soil supporting the footing. The problem formulated, as shown in Fig. 2, has been solved by Al-Aghbari [3] using the theory of plasticity.

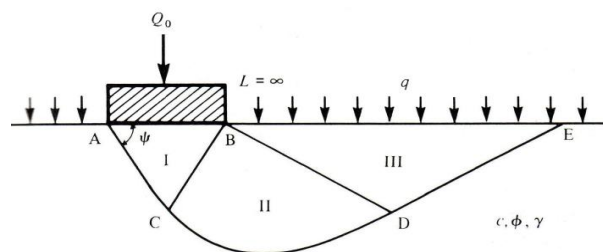


Fig. 2 Failure Wedge (after [2])

The basic solution available indicated that the failure pattern should consist of three zones; (I, II, III), where zone (I) is an active Rankin zone, which pushed the radial Prandtl zone (II) sideways and the passive Rankin zone (III) in an upward direction. The lower boundary (ACDE) of the displaced soil mass is composed of two straight lines AC and DE, inclined at  $45 + \phi/2$  and  $45 - \phi/2$  respectively, to the horizontal. The shape of the connected curve CD depends on the angle  $\phi$  and on the ratio  $\gamma B/q$ .

When  $\gamma B/q$  approaches 0 (weightless soil) the curve becomes a logarithmic spiral, which for  $\gamma = 0$  degenerates into a circle. In the general case ( $\gamma B \neq 0$ ), the curve lies between a spiral and circle as long as ( $\phi \neq 0$ ). For frictionless soil ( $\phi = 0$ ), the curve is always a circle. All these finding have been

Tahsin Toma Sabbagh is with the School of Computing, Science and Engineering, University of Salford, UK (e-mail: t.toma@salford.ac.uk).

Ihsan Al-Abboodi and Ali Al-Jazaairry are with the School of Computing, Science and Engineering, University of Salford, UK.

confirmed experimentally by Vesic [4].

A closed analytical solution of this problem has not yet been found and probably will not be found, except for special cases. For weightless soil ( $\gamma = 0$ ), Prandtl and Reissner have found that:

$$q_o = CN_c + qN_q \quad (1)$$

where  $N_c$  and  $N_q$  are dimensionless bearing capacity factors defined by:

$$N_q = e^{(\pi \tan \phi)} \tan^2 (\pi/4 + \phi/2) \quad (2)$$

$$N_c = (N_q - 1) \cot \phi \quad (3)$$

For cohesionless soil without overburden ( $C = 0$ ,  $q = 0$ ), it can be shown that:

$$q_o = \frac{1}{2} \gamma B N_\gamma \quad (4)$$

where  $N_\gamma$  varies sharply with the dilatancy angle ( $\psi$ ), Vesic [4] showed that the value of  $N_\gamma$  can be approximated with an error on the safe side (not exceeding 10% for  $15 < \phi < 45$  and not exceeding 5% for  $20 < \phi < 40$ ) by the analytical expression:

$$N_\gamma = 2(N_q + 1) \tan \phi \quad (5)$$

For all intermediate cases, where  $C \neq 0$ ,  $q \neq 0$ ,  $\gamma \neq 0$  (1) and (4) are combined into:

$$q_o = CN_c + qN_q + \frac{1}{2} \gamma B N_\gamma \quad (6)$$

This equation is known as Busiman-Terzaghi equation. This superposition is not strictly correct; however, it leads to errors which are on the safe side, not exceeding 17-20% for  $\phi = 30^\circ$  to  $40^\circ$ , while equal 0 for  $\phi = 0^\circ$

It should be mentioned that in the literature there exists a great variety of proposed solutions to this problem. While, the variations in  $N_c$  and  $N_q$  values proposed remain relatively insignificant, the differences in  $N_\gamma$  values coming primarily from the sharp variation of  $N_\gamma$  with the dilatancy angle ( $\psi$ ), which are substantial, ranging from about one-third to double the values from (6) [5].

## II. PREVIOUS STUDIES

The behaviour of axially loaded skirted shallow foundations resting on sand was studied by Hisham [6], using numerical analysis. The effects of foundation size, shear strength of sand, and confinement depth on bearing capacity and settlement of skirted foundations were investigated. The results revealed that skirted foundations exhibit bearing capacity and settlement values that are close to those of pier foundations of the same width and depth. Moreover, the enhancement in bearing capacity of shallow foundation increases with the increase of confinement depth and decreasing relative density of sand. Settlement reduction factor of more than 70% was noticed in the case where skirt depth to foundation width of 2.0 was reached.

Shabana and Joseph [7] presented results for square footings with and without confinement on uniform soil condition showing that the bearing capacity can be improved by a factor of 1.08 to 1.64 when confinement was provided with depth to width of footing ratio of 0.25 to 1.0.

Azzam and Farouk [8] studied laboratory model tests and performed a numerical study on the behaviour of a strip footing with structural skirts adjacent to a sand slope with different skirt depths, different locations of the skirted footing relative to the slope crest and the slope inclination. They concluded that stabilizing the earth slope using structural skirts with adequate depth in the vicinity of strip footing adjacent to slope crest has a significant effect in improving the soil bearing capacity.

Nazir and Azzam [9] investigated a circular type of footing resting on sand pile-partially replaced for two cases: with and without surrounding skirts. Their results showed an improvement of the bearing capacity and a remarkable decrease in vertical settlement.

El-Sawwaf [10] conducted tests of model footings resting on sandy soil to study the confinement effect on the behaviour of such footings. Testing parameters under study included depth of soil and cell dimensions (height, diameter). The results revealed that the bearing capacity of circular footing can be appreciably increased by soil confinement.

Cerato [11] carried-out model footing tests on a finite layer of granular soil. The bearing capacity of model footings resting on the surface of a finite layer of granular (cohesionless) soil was investigated. Results of the model scale footing tests showed that the modified bearing capacity factor,  $N_\gamma$ , is dependent on both relative density ( $D_r$ ) and relative layer thickness ( $H/B$ ) but appears to be independent of footing shape.

Anderson [12] studied the collapse of saturated soil due to reduction in confinement. The potential for collapse due to a reduction in confinement is evaluated for two very different soils: uniformly graded sand and an undisturbed clayey colluvium soil. Soil specimens were consolidated anisotropically and subjected to constant-shear-drained (CSD) tests. During the CSD test, the effective confining pressure is gradually reduced while the shear stress is held constant. It was depicted from the study that only for very loose specimens collapse was observed before the failure envelope or steady state is reached. In general, specimens subjected to the CSD stress path behaved differently compared to specimens of similar initial density and confining pressure subjected to typical compression stress paths. This implies that predicting the collapse potential of the stress path is of great importance and hence the potential flow failure of such soils.

## III. THE CASE STUDY

As a case study, the adopted building for this research is an existing building (Al-Samirai complex in Baghdad), consists of two floors and has a spread type of foundation resting on a sandy clay soil. The thickness and depth of the spread foundations are 0.6 m each, and the foundation is enduring a uniformly distributed load of (75 kN/m<sup>2</sup>). The subsoil

consisted of a deposit of sand layer of 20 m thickness. The properties of the adopted sand ( $\gamma = 17 \text{ kN/m}^3$ ,  $\nu = 0.3$ ,  $E = 40000 \text{ kPa}$ ). The ground water table is assumed to be at great depth below the ground surface. The building foundation is simulated with a plate element of 0.6 m thickness; its properties are  $EA = 105 \text{ kN/m}$  and  $EI = 9000 \text{ kN/m}^2/\text{m}$ , whereas the sheet piles (confinement) are simulated as elastic material with plate thickness of 0.02 m and properties of  $EA = 5 \times 10^6 \text{ kN/m}$ ,  $EI = 21.875 \text{ kN/m}^2/\text{m}$ . The plane strain model was used with the 8 node element. The mesh was generated by the program and refined in the area around the footing.

#### IV. NUMERICAL MODELLING AND ELEMENT TYPE

The geometry of the finite element soil model adopted for the analysis is shown in Fig. 3. It is believed that a 3-D analysis is the best representations for rafts and piled raft foundations. In this study, a finite element (ANSYS) software is used and a three dimensional plane strain analysis is carried out.

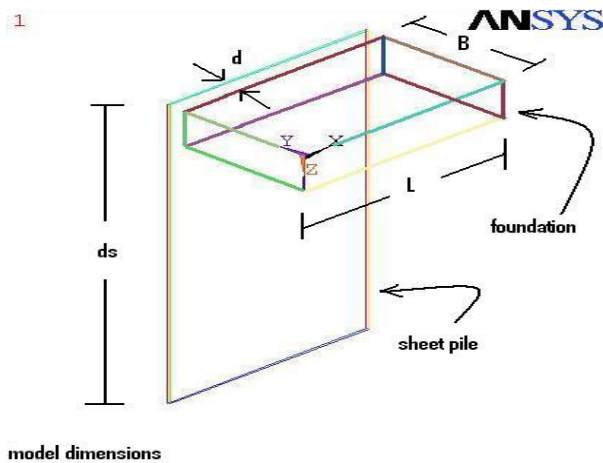


Fig. 3 Model Dimensions

The spread foundation was modelled as a plate element with the appropriate geometrical parameters and geometrical boundaries as suggested by Prakoso and Kulhawy [13]. Nonlinear material behaviour is adopted for the soil in which a Drucker-Prager model is used to represent the nonlinearity behaviour of the problem. Sparse direction solution method is carried out to solve the non-linear equilibrium equations. Solid 45 brick element is used for the modelling of soil; the element is defined by eight nodes having three degrees of freedom at each node. The problem includes three materials soil, concrete, and steel, as shown in Table I. Two types of elements are selected; Solid65 for concrete foundation and Solid45 for soil and sheet pile.

TABLE I  
MATERIALS PROPERTIES

Materials	E (N/m <sup>2</sup> )	$\mu$	C (N/m <sup>2</sup> )	$\Phi$ (°)	$\gamma$ kN/m <sup>3</sup>
Sandy clay	$45.2 \times 10^6$	0.4	15	43	20
Steel	$200 \times 10^9$	0.3	-	-	77
Concrete	$20 \times 10^9$	0.15	-	-	25

#### V. YIELD CRITERIA

The plasticity theory provides a material mathematical relationship that characterizes the elasto-plastic response of materials. The yield criterion determines the stress level at which yielding is initiated. For multi component stress, this is represented as a function of the individual components,  $f(\{\sigma\})$ , which can be interpreted as an equivalent stress ( $\sigma_e$ ):

$$\sigma_e = f(\{\sigma\}) \quad (7)$$

where  $\{\sigma\}$  = Stress vector

When the equivalent stress is equal to material yield parameter ( $\sigma_y$ ):

$$f(\{\sigma\}) = \sigma_y \quad (8)$$

The material will develop plastic strain. If ( $\sigma_e$ ) is less than ( $\sigma_y$ ), the material is elastic and the stress is developed according to the elastic stress-strain relationship.

The Drucker-Prager model is used for soil as yield criteria, which is applicable to granular (frictional) material such as soil and concrete, and uses the other cone approximation to the Mohr-Coulomb law. The input consists of only three constants: the cohesion value (C), the angel of internal friction ( $\phi$ ), and the dilatancy angle ( $\psi$ ). The constants have the following values for each condition type:

a. For triaxial compression problem:

$$k = \frac{6 \times C \times \cos \phi}{\sqrt{3} \times (3 - \sin \phi)} \quad (9)$$

$$\alpha = \frac{2 \times \sin \phi}{\sqrt{3} \times (3 - \sin \phi)} \quad (10)$$

b. For plane strain problem:

$$k = \frac{\tan \phi}{\sqrt{9 + 12 \times \tan^2 \phi}} \quad (11)$$

$$\alpha = \frac{\tan \phi}{\sqrt{9 + 12 \times \tan^2 \phi}} \quad (12)$$

#### VI. LOAD APPLICATION AND BOUNDARY CONDITIONS

Sparse direction solution method is adopted, which is normally used for static and full transient, and also for linear and non-linear solution. Static analysis type is adopted as a structural analysis and because of non-linear soil behaviour, the load step file method is chosen. The modelling output, meshing the model, applied loads at the foundation nodes; deformed shape, average displacement, and plastic strain are shown in Figs. 4-8.

The study focused on two main variables: i-distance between sheet pile and footing edge (d), ii-depth of sheet pile (ds). Those main variables were performed under different foundation dimensions ( $B \times L$ ). The results of node 228 (under

the footing centre line) were taken as the representing outcome of the study.

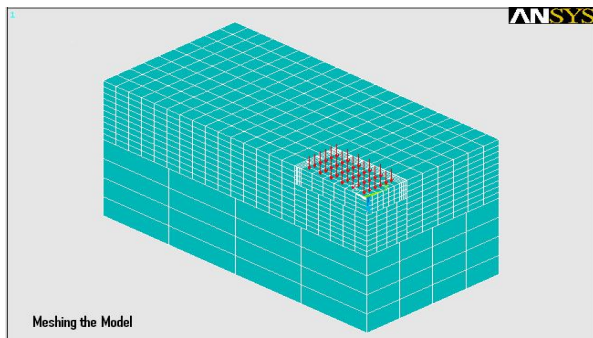


Fig. 4 Meshing the Model

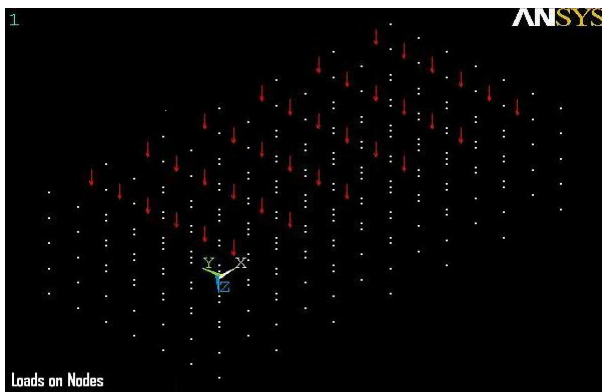


Fig. 5 Applied Loads at the Foundation Nodes

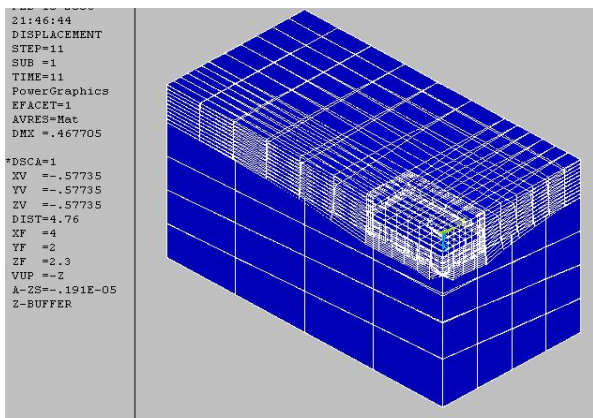


Fig. 6 Deformed Shape

#### A. Effect of Distance between Sheet Pile and Edge of the Footing ( $d$ )

Three values of ( $d$ ) are included, i.e. 0.1 B, 0.5 B, 0.75 B, where (B) is the short dimension of the foundation.

From Figs. 9 (a) and (b), it can be seen that the deviator stress ratio increase with increasing the value of  $d/B$  until reaching a peak value at  $d/B = 0.5$ . This holds for all depths of sheet piles. This behaviour can be explained by the relative load concentration on the available contact area i.e. at  $d/B$  the

load concentration will be high due to increase in the confining pressure. Increasing the ratio ( $d/B$ ) gradually lead to an increase in the deviator stress (twice the diameter of Mohr circle); the optimum value of  $d/B$  is 0.5, after this point the trend of the curve changes as the confinement start release, and hence, the deviator stress decreases with increasing the ratio ( $d/B$ ).

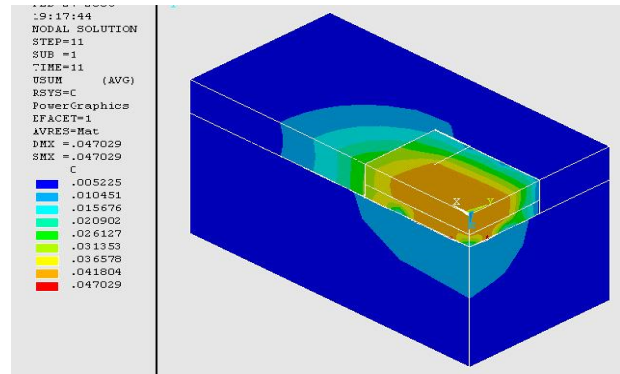


Fig. 7 Average Displacement

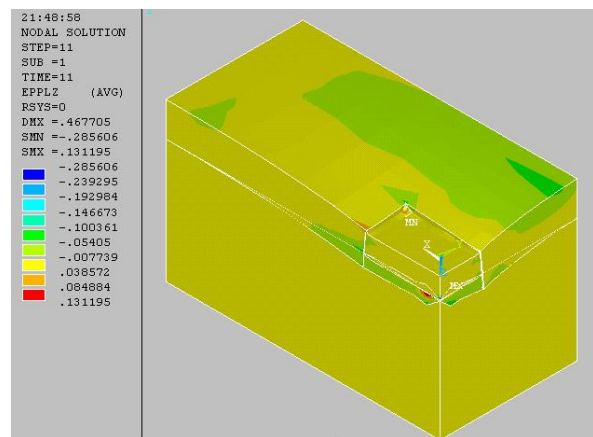


Fig. 8 Plastic Strain

From Figs. 10 (a) and (b), the values of vertical displacement ( $U_z$ ) at the first part of the curve is decreased gradually until it reached a minimum value at  $d = 0.5 B$ . After this point, the value of ( $U_z$ ) increases with increasing the distance ( $d$ ). This behaviour came as a result of increasing the stiffness of soil at the first part of the curve due to the action of confinement.

#### B. Effect of Sheet Pile Depth ( $d_s$ )

Three values of sheet pile depths were attempted in this study, these are: 0.5 B, 0.1 B and 1.5 B. Figs. 11 (a) and (b) show the relationship between the deviator stress ( $\sigma_1 - \sigma_3$ ) and the vertical displacement ( $U_z$ ). It can be shown that the deviator stress decreased with increasing the depth of sheet pile. This behaviour is due to the increase in the confinement stress ( $\sigma_3$ ), which as a result, implicit a decrease in the deviator stress ( $\sigma_1 - \sigma_3$ ).

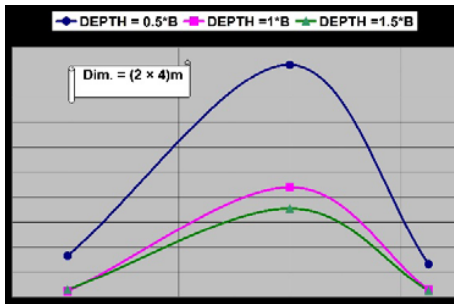


Fig. 9 (a) Load-Distance Relationship for (2×4) m Foundation

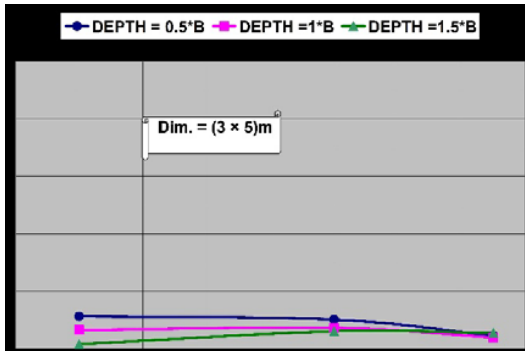


Fig. 9 (b) Load-Distance Relationship for (3×5) m Foundation

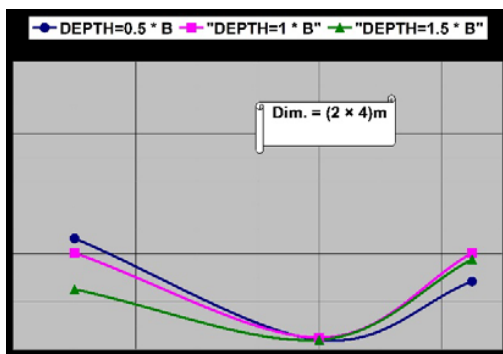


Fig. 10 (a) Vertical Displacement-Distance Relationship for (2×4) m Foundation

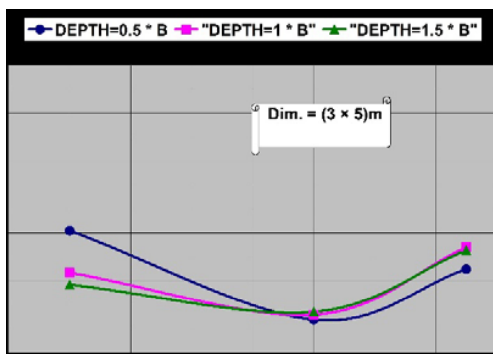


Fig. 10 (b) Vertical Displacement-Distance Relationship for (3×5) m Foundation

Figs. 12 (a) and (b) illustrate the reduction of the stresses with the depth of sheet piles compared to those without the presence of sheet piles. The stresses are clearly decreased with a corresponding increase in the depth of sheet pile with a ratio ranging from 0.65 to 0.1, depending on the distance ( $d$ ).

Finally, Figs. 13 (a) and (b) depict the distance-vertical displacement relationship with and without confinement for both foundation types, i.e. (2×4) m, (3×5) m. It can be seen that the effect of confinement is clearly reduced with the increase of foundation dimensions.

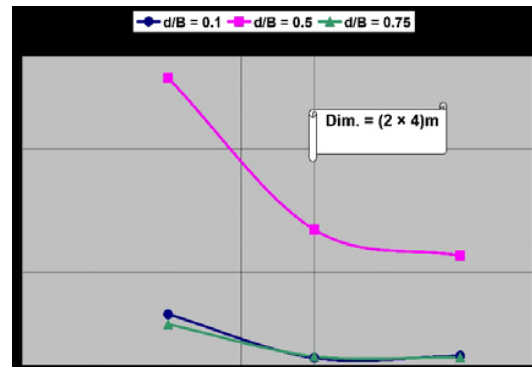


Fig. 11 (a) Load-Sheet Pile Depth Relationship for (2×4) m Foundation

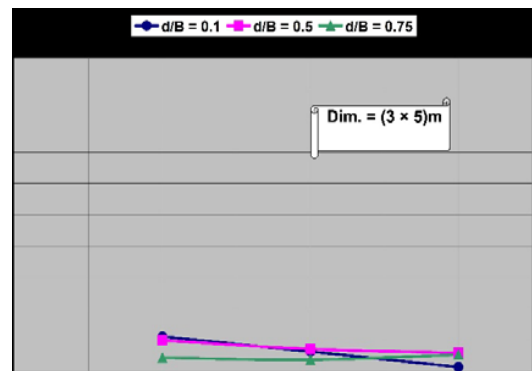


Fig. 11 (b) Load-Sheet Pile Depth Relationship for (3×5) m Foundation

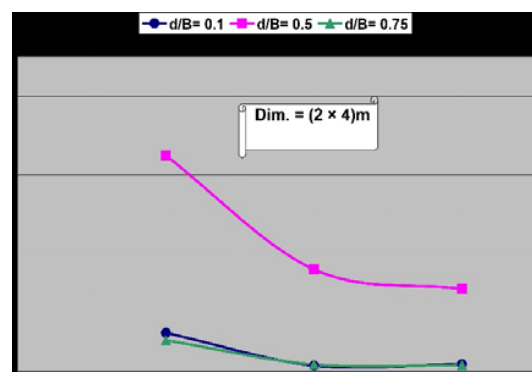


Fig. 12 (a) Stress-Sheet Pile Depth Relationship for (2×4) m Foundation



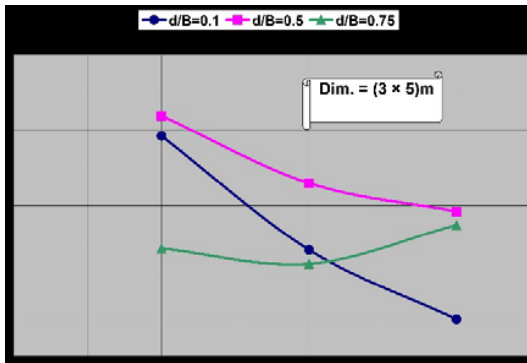


Fig. 12 (b) Stress-Sheet Pile Depth Relationship for (3×5) m Foundation

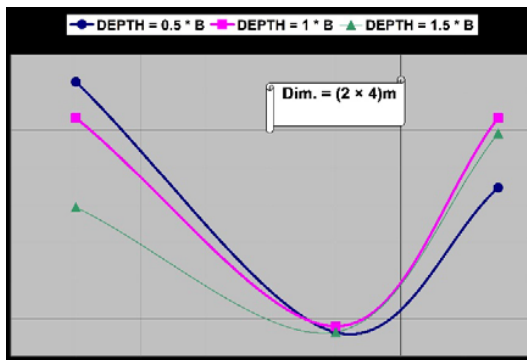


Fig. 13 (a) Distance-Vertical Displacement Relationship with and without Confinement for (2×4) m Foundation

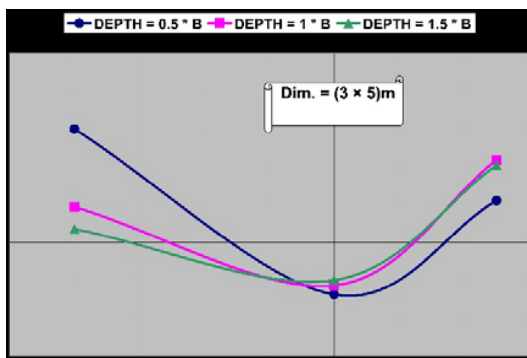


Fig. 13 (b) Distance-Vertical Displacement Relationship with and without Confinement for (3×5) m Foundation

## VII. CONCLUSIONS

Implementing confinements around and below foundations strengthens the underlying soil and generates a soil resistance. This leads to an improvement in their performance. Conclusions with regard to the numerical results obtained for foundations with different dimensions and different sheet pile distances from the foundation edge can be drawn below:

1. Soil confinement has a significant effect on improving the behaviour of spread footing on cohesionless soil.
2. Thus, finite element analysis presented in this study helped in better understanding and identifying the failure

pattern of spread foundations with and without confinement.

3. The confinement of soil layer under the foundation has proven to be very effective to increase soil strength and reduce the deviator stress within the soil mass by 65% in comparison with the deviator stress under the same foundation, the same soil and same load level but without confinement.
4. The confinement of soil under spread foundations reduces the vertical displacement by about 90%.
5. The optimum value of  $d$  (distance between the sheet pile and the foundation edge) is found to be  $0.5 B$ .
6. The effect of confinement is reduced with the increase of foundation dimensions.

## REFERENCES

- [1] Lambe W T & Whitman R V (1969), "Soil Mechanics", 2nd edition, John Wiley & Sons, NY.
- [2] Winterkorn H F (1975), "Foundation Engineering Hand Book" Van Nostrand Reinhold Co.
- [3] Al-Aghbari M Y (2007), "Settlement of Shallow Circular Foundations with Structural Skirts Resting on Sand", the Journal of Engineering Research Vol. 4, No.1, 11-16.
- [4] Vesic A (1963), "Bearing capacity of deep foundations in sand" Highway research Record, No. 39.
- [5] Frydman S and Burd H J (1997), "Numerical Studies of Bearing Capacity Factor  $N_\gamma$ ", Journal of Geotechnical and Geoenvironmental Engineering, Vol. 123, No.1, 20-29.
- [6] Hisham T E (2013), "Bearing Capacity and Settlement of Skirted Shallow Foundations on Sand" International Journal of Geomechanics, ASCE, Vol. 13, No.5, 645–652.
- [7] Shabana S K and Joseph M (2010), "Effect of Structural Skirt on Square Footing" <http://117.211.100.42:8180/jspui/bitstream/123456789/1063/1/CEGE10.pdf>.
- [8] Azzam W R and Farouk A (2010), "Experimental and Numerical Studies of Sand Slopes Loaded with Skirted Strip Footing", Electronic Journal of Geotechnical Engineering, Vol. 15 No.3, 795-812.
- [9] Nazir A K and Azzam W R (2010), "Improving the bearing capacity of footing on soft clay with sand pile with/ without skirts", International Review of Civil Engineering Journal, Vol.1, No.1, 32-38. doi: 10.1016/j.aej.2010.06.002.
- [10] El-Sawwaf M (2005), "Behavior of circular footing resting on confined granular soil", Journal of Geotechnical and Geoenvironmental Engineering, ASCE, 131 (3), 359-366.
- [11] Cerato A B (2000), "Model footing test on finite layer of granular soil" graduate research assistant, university of Massachusetts, Amherst, USA 2000.
- [12] Anderson S A (1995), "Collapse of saturated soil due to reduction in confinement" Journal of Geotechnical Engineering, Vol. 121, No. 2, 216-220.
- [13] Prakoso W A and Kulhawy F H (2001), "Contribution to Piled Raft Foundation Design Journal of Geotechnical and Geoenvironmental Engineering", ASCE, 127(1), 17-24.